Effect of Mineral Particles Containing Iron on Primary Cultures of Rabbit Tracheal Epithelial Cells: Possible Implication of Oxidative Stress

Catherine Guilianelli,[1] Armelle Baeza-Squiban,[1] Emmanuelle Boisvieux-Ulrich,[1] Odile Houcine,[1] Roger Zalma,[2] Christiane Guennou,[2] Henri Pezerat,[2] and Francelyne Marano[1]

[1]Laboratoire de Cytophysiologie et Toxicologie Cellulaire, Université de Paris VII, 75005 Paris, France; [2]Laboratoire de Réactivité de Surface et Structure, Université P. et M. Curie, 75005 Paris, France

Environmental mineral particles such as asbestos are responsible for numerous respiratory diseases. In addition to effects related to their geometry, particles are now assumed to act by triggering an oxidative stress process. Iron-containing particles, in particular, can produce oxygen-activated species by oxidizing their iron. To evaluate the involvement of iron-containing particles in respiratory diseases, three mineral particles (chrysotile, nemalite, and hematite) were tested in primary cultures of tracheal epithelium. Because of the ciliary beat, the three mineral particles were quickly concentrated at the periphery of the mucociliary epithelium, reconstituted *in vitro* where they induced cellular lesions. Endocytosis of the three types of particles was observed. Cytotoxicity studies have indicated that among the tested particles, the most cytostatic after 24 hr of treatment was the one that contained more Fe^{2+} available on the surface, nemalite. Moreover, the effect of nemalite was reduced by pretreatment with desferrioxamine. As mineral particles, especially asbestos, are suspected to induce squamous metaplasia, we chose to study two specific transformations of the epithelium: the expression of cytokeratin-13 and the formation of cross-linked envelopes. Under our culture conditions, nemalite and chrysotile increased the expression of the cytokeratin-13, a specific marker of squamous metaplasia, whereas nemalite was the only particle able to strongly induce the formation of cross-linked envelopes. Nemalite was the most cytostatic particle and the most efficient at inducing squamous metaplasia. Measures of oxidizing power by electron-spin resonance revealed that nemalite produced the most oxygen-activated species. This observation and its reduced toxicity by the desferrioxamine treatment suggest that nemalite could act on rabbit tracheal epithelial cells by an oxidative stress process. *Key words:* cytotoxicity, iron-containing mineral particles, oxygen-activated species, phagocytosis, primary cultures, squamous metaplasia, tracheal epithelial cells. *Environ Health Perspect* 101:436–442(1993)

It has been known for many years that exposure to airborne asbestos fibers can lead to diseases such as asbestosis, lung cancer, and mesothelioma. As a result, asbestos is the most-studied natural mineral fiber. Although the exact mechanism of toxicity of mineral particles is unknown, several hypotheses have been proposed. The first one involves the fibrous nature of the mineral, its length, and its diameter (*1–3*). However, other studies carried out with fibers of equal length and diameter demonstrated that characteristics other than fiber size, such as chemical composition, are also crucial determinants of fiber toxicity (*4,5*). To explain this last point, Zalma et al. (*6*) and Pezerat (*5*) proposed a mechanism by which an interaction between an electron donor site (at the liquid–solid interface of the particle) and molecular oxygen present at a constant concentration in biological medium could exist, leading to the formation of electrophilic entities (A*), responsible for the oxidative stress. These oxidative species include OH radicals and iron oxo [Fe(V)] (*7,8*), which are apt to react with some biological molecules. Mineral particles have an oxidizing power dependent on the quantity of accessible divalent iron.

The production of oxygen-activated species (OAS) by mineral particles described by physicochemists has also been suspected by biologists. Mossman and Landesman (*9*) thought that OAS were involved in asbestos toxicity. This was emphasized by observations that asbestos toxicity can be reduced by co-treatment of asbestos fibers with antioxidant (*10*).

Our purpose is to contribute to the understanding of the toxicity of mineral particles on the respiratory epithelium, which is the main epithelial target of these compounds. The role of oxidative stress provoked by iron-containing mineral particles was also investigated. For this purpose, we used an *in vitro* model of mammal airway epithelium obtained by the explant technique (*11*). This *in vitro* model allows us to maintain the cellular polarity and differentiation as found in intact tissue and to eliminate confounding immunological and nervous influences. Three mineral particles have been tested so far: nemalite, the richest Fe^{2+}-containing mineral, Canadian chrysotile, an asbestos form naturally contaminated by nemalite and magnetite, and hematite containing Fe^{3+}. Although these three naturally occurring particles have different shapes, we chose to use samples of particles, whose sizes were compatible with phagocytosis.

To measure the toxic potential of these particles on the respiratory epithelium, established cytotoxic tests of acute toxicity for this culture model (*12,13*) have been used, thus leading to further study of a more specific effect on the epithelium, the induction of squamous metaplasia. Squamous metaplasia is characterized by conversion of mucociliary cells to keratinizing cells and is a putative preneoplastic lesion; it has been shown to occur in rodent and human tracheobronchial cells in organ culture after exposure to asbestos (*14*). The mechanical injury induced by asbestos fibers was first considered to be responsible for the development of squamous metaplasia (*10*). However, new data suggest that OAS produced by particles can also be responsible for this pathological differentiation (*15*). In these studies the induction of squamous metaplasia by mineral fibers or OAS has principally been evaluated by morphological observations. So we have followed the induction of squamous differentiation through two criteria: the evolution of the expression of cytokeratins and the formation of cross-linked envelopes, the ultimate stage of squamous metaplasia. To evaluate the involvement of OAS in rabbit tracheal epithelial (RTE) cell toxicity, spin-trapping and electron spin resonance (ESR) spectroscopy were used to detect the formation of oxidizing species from the mineral particles.

Materials and Methods

We removed tracheas from 1-month-old Fauve de Bourgogne rabbits. The epithelium was separated from the underlying cartilage and cut into 2-mm^2 explants (*11*). The explants were grown on a thick, hydrated gel of collagen, supplemented with minimal essential medium (MEM, Gibco) and 10% fetal calf serum (*11*). At the beginning of the culture, cells are covered with MEM containing 10% fetal calf

Address correspondence to C. Guilianelli, Laboratoire de Cytophysiologie et Toxicologie Cellulaire, Université de Paris 7, Tour 53-54, 3eme étage, case 70 73, 75 251, Paris cedex 05 France.
We thank F. Meury, Laboratoire d'Anatomie Comparée, for valuable technical assistance with the scanning electron microscope and M. J. Falxa for technical assistance. This work was supported by grants from DRED, Action spécifique toxicologie de l'environnement, and MRE 91C0543 and 91739.
Received 8 March 1993; accepted 23 July 1993.

serum, supplemented with epidermal growth factor (EGF; 25 ng/ml), transferrin (5 µg/ml), glutamin (5 µg/ml), insulin (5 µg/ml), and hydrocortisone (92 µg/ml). At the time of treatment with particles, serum and transferrin are not added to MEM.

A Canadian chrysotile sample [$Mg_3SiO_5(OH)_4$] was obtained from the Union Internationale Contre le Cancer. This chrysotile is contaminated by nemalite (about 5%) and magnetite (Fe_3O_4). The proportion of Fe^{2+}, expressed as FeO, is 1.44%. Chrysotile consisted of long and flexible fibers, which in aqueous solution dissociated into thinner ones. A length distribution was impossible to determine because of the heterogeneity of these fibers.

Nemalite (Asbestos, Quebec) is a fibrous brucite [$Mg(OH)_2$] in which 8% of the Mg^{2+} is substituted by Fe^{2+}. Nemalite fibers were ground for an hour in a mechanical crusher. The distribution of fiber sizes was from 1 µm for the smaller ones to 15 µm for the longer ones.

Hematite (Fe_2O_3) is a commercial compound (Merck) which contains Fe^{3+}. Hematite is composed of round particles about 1 µm in diameter. Minerals at different concentrations were suspended in serum-free culture medium by sonication and vortexing and immediately added to cultures. For all experiments, each concentration of minerals was systematically tested on three culture dishes.

In some experiments, particles were preincubated either with 10 mM desferrioxamine [1-amino-6,17-dihydroxy-7,10,18,21-tetraoxo-27-(*N*-acetylhydroxylamino)-6,11,17,22-tetraazaheptaeicosane; Desferal, Ciba-Geigy] in MEM or with only MEM for 4 hr at 37°C. The particles were then spun down and excess desferrioxamine removed by washing with MEM. Before the addition of the particles to the cultures, we resuspended particles in MEM supplemented with growth factor.

Once outgrowths were established, we fixed cultures in 2% glutaraldehyde in 0.05 M cacodylate buffer (pH 7.4) for 1 hr. After rinsing in 0.1 M fixation buffer, the samples were postfixed for 1 hr in 1% OsO_4 in the same buffer. The samples were dehydrated with a graded series of ethanol and then either embedded in Epon or critical-point dried using CO_2 in a Balzers apparatus. We coated the critical-point dried samples with about 40 nm gold and examined them with a JEOL JMS 6100 scanning electron microscope. Semithin sections of embedded samples were cut with a diamond knife on an LKB ultramicrotome. We stained 1-µm semithin sections with methylene and azur II blue and then viewed them on a Nikon optiphot microscope.

We applied particles in a single dose and in various concentrations on day 7 and carried out viability measurements 24 hr after treatment. Two viability assays, indicative of membrane damage, were used. The first method involved measuring the release of cellular lactate dehydrogenase and was performed as previously described (*12*). Membrane damage was also assessed by the exclusion of trypan blue from cells.

We evaluated culture growth by an image analysis system. Cultures were filmed daily and then the images were analyzed by a microcomputer 386 AT equipped with an image-processing card PIP 1024 B (Matrox, Jorval, Canada). We determined the culture growth by measuring the ratio of outgrowth surface to explant surface (*11*). Surface ratios of treated cultures were expressed as a percentage of control culture values. Particles were applied in various concentrations on day 2 of culture, and inhibition of growth was determined on days 3, 4, and 7.

To detect the induction of squamous differentiation, we used a modification of the method of Sun and Green (*16*) to evaluate cornified envelope formation. Briefly, cells were removed from the culture dish with 0.05% trypsine-0.7mM EDTA (Gibco) and counted in a hemocytometer to determine total cell number. Cells were then centrifuged, the pellet resuspended in 20 mM dithiothreitol and 2% sodium dodecylsulfate (SDS), heated to 100°C for 10 min, and the remaining cornified envelopes counted in hemocytometer. The data are expressed as number of cross-linked envelopes (CLE) divided by the total cell number times 100. We determined CLE formation for 16-day-old cultures treated for 13 days with particles at 10 µg/cm^2.

Keratin intermediate filaments characterizing epithelial cells were revealed by indirect immunofluorescence of cultures treated for 7 days at 20 µg/cm^2. Double labeling was performed, coupling the detection of the whole keratins with a polyclonal antikeratin (Sigma Co, St. Louis, Missouri) and the detection of specific cytokeratins with monoclonal antibodies. We removed the medium and fixed cells *in situ* with cold methanol for 20 min at -20°C. The cells were then treated for 5 min with acetone at -20°C and washed with PBS-2% bovine serum albumin (BSA). We then incubated the permeabilized cells for 1 hr at 37°C in guinea pig antikeratin (Sigma) and monoclonal anticytokeratin-13, 1C7 (ICN; Immuno-Biologicals, Chemical Credential, Costa Mesa, California), at 1:100 and 1:10 dilution, respectively, in PBS-BSA. After washing with PBS-BSA, we treated the cells with affinity-purified goat antiguinea pig IgG-rhodamine (Jackson Immunoresearch, West Grove, Pennsylvania) and with goat antimouse IgG-fluorescein isothiocyanate (Sigma) diluted 1:200 and 1:128, respectively, in PBS-BSA for 1 hr in the dark at room temperature. The cells were washed thoroughly in PBS-BSA, cover slipped using a nonfluorescent mounting medium, and examined using a Nikon optiphot microscope equipped for epifluorescence. Photographs were made using Tura chroma film.

After 10 days of growth of tracheal cells treated with particles for 8 days at 50 µg/cm^2, the total cell population was removed from the culture dishes by collagenase treatment (0.2% in MEM at 37°C). After centrifugation, we washed the cells twice with PBS and subsequently extracted for keratins according to the technique described by Achtstaetter (*17*). In brief, after thorough homogenization of cells in a detergent buffer [10 mM Tris-HCl, 140 mM NaCl, 5 mM EDTA, 1% (w/v) Triton X-100, pH 7.6] at 4°C, the pellet obtained by centrifugation at 14,000*g* was resuspended in a high-salt buffer [10 mM Tris-HCl, 140 mM NaCl, 1.5 M KCl, 5 mM EDTA, 0.5% (w/v) Triton X-100, pH 7.6] and incubated for 30 min at 4°C. The high-salt buffer insoluble material obtained as a pellet after centrifugation was extracted a second time in the same buffer and washed twice with 10 mM Tris-HCl (pH 7.6) and stored at -20°C until use. The three buffers were supplemented with 5 mM dithiothreitol, 1 mM benzamidine, and 1 mM phenylmethylsulfonyl fluoride. The pellet of the remaining insoluble material was dissolved in SDS-sample buffer (0.0625 M Tris-HCl, pH 6.8, 3% SDS, 10% glycerol and 5% ß-mercaptoethanol) by heating, and any insoluble material was removed by centrifugation.

We electrophoretically separated keratin proteins in one-dimensional SDS-10% polyacrylamide gels. After electrophoresis, proteins were blotted on nitrocellulose paper according to Towbin et al. (*18*). We reacted blotted proteins with monospecific antibody: anticytokeratin-13, ICN. Keratin bands were immunologically stained by the method outlined by the reagent supplier (Enhanced ChemiLuminescence kit, Amersham International plc, UK) using peroxidase-conjugated (Pierce, Rockford, Illinois) goat antimouse IgG (H+L) .

The electrophilic species, A*, are able to extract a hydrogen atom from an RH molecule to give an R radical. This capacity is used to evaluate the oxidizing power. In our test, the RH molecule is the formate anion, $HCOO^-$, which produces the carboxylate radical anion, $CO_2^{\cdot-}$. The very short life of the radicals $CO_2^{\cdot-}$ requires a spin-trapping agent, 5,5'-dimethyl-1-pyroline-N-oxide (DMPO), which reacts with $CO_2^{\cdot-}$ to give the radical adduct (DMPO–$CO_2^{\cdot-}$),

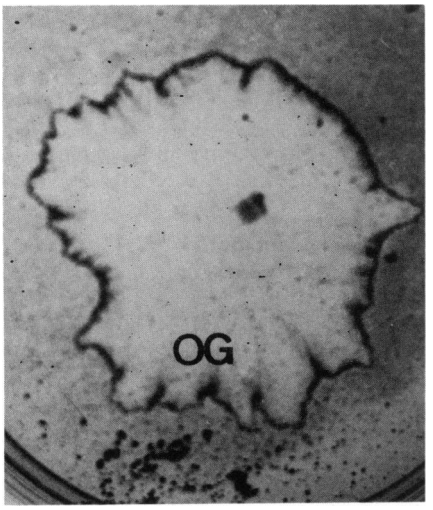

Figure 1. Photograph of an 8-day-old primary culture of rabbit tracheal epithelial cells treated with hematite (100 μg/cm^2) for 6 days. Note the accumulation of particles at the periphery of the outgrowth (OG) resulting from the ciliary beat (2.5×).

which has a half-life time of about 1 hr under our experimental conditions. The quantification of the oxidizing power is evaluated by the intensity of the ESR signal corresponding to the radical adduct (Varian CSE 109 ESR spectrograph). In our study, fibers or particles (45 mg) were in suspension in MEM (2 ml) containing a phosphate buffer (1 M) at 37°C in a dark reactor. DMPO–$CO_2^{\cdot}$ is identified from its characteristic ESR signal at g = 2.0055 with the following coupling constants: a_N = 15.6 G, a_H = 19.0 G.

Results

Morphological Modifications after Treatment with Particles

The primary culture was established by migration of cells from the original piece of epithelium, forming a halo around the explant. The outgrowth appeared within 3 days, reconstituting a stratified epithelium with both basal and differentiated cells. Functional ciliated cells persisted for the complete duration of the culture (*19*).

Before depositing them on cultures, we shook particles vigorously to achieve homogeneous distribution of the particles on the culture. However, because of the ciliary beat, particles are swept from the outgrowth surface, and after 24 hr most of them were concentrated at the periphery of the culture, as shown on Figure 1. On the rest of the outgrowth, particles were heterogeneously scattered and were probably strongly adherent to the cell surface because the numerous washings required for the preparation of scanning microscopy samples were not sufficient to wash them off.

Alterations induced by particles on cells were examined by scanning electron microscopy. As suspected by the number of particles observed at the peripheral of the outgrowth, peripheral cells exhibited dramatic modifications. In contrast, the cells of the rest of the outgrowth seemed to preserve their integrity. Particularly, cilia of ciliated cells did not exhibit lesions, although they have been strongly implicated in the removal of particles at the beginning of the treatment.

Hematite particles formed conglomerates at the surface of the outgrowth (Fig. 2c). Figure 2d shows the profound modifications induced by hematite on RTE cells. Some cells were distorted, exhibiting blisters and swelling. Such swelling of the apical surface of cells suggested endocytosis.

Cultures treated with fibers (nemalite and chrysotile) did not show cells as swollen as those observed after treatment with hematite. But numerous small, round cells appeared at the periphery of the outgrowth, corresponding to cells that are sloughing off the tissue (Fig. 2e). Nemalite fibers as well as chrysotile fibers pitted cells (Fig. 2b,e), probably penetrating into them. An observation at higher magnification revealed that some other long fibers

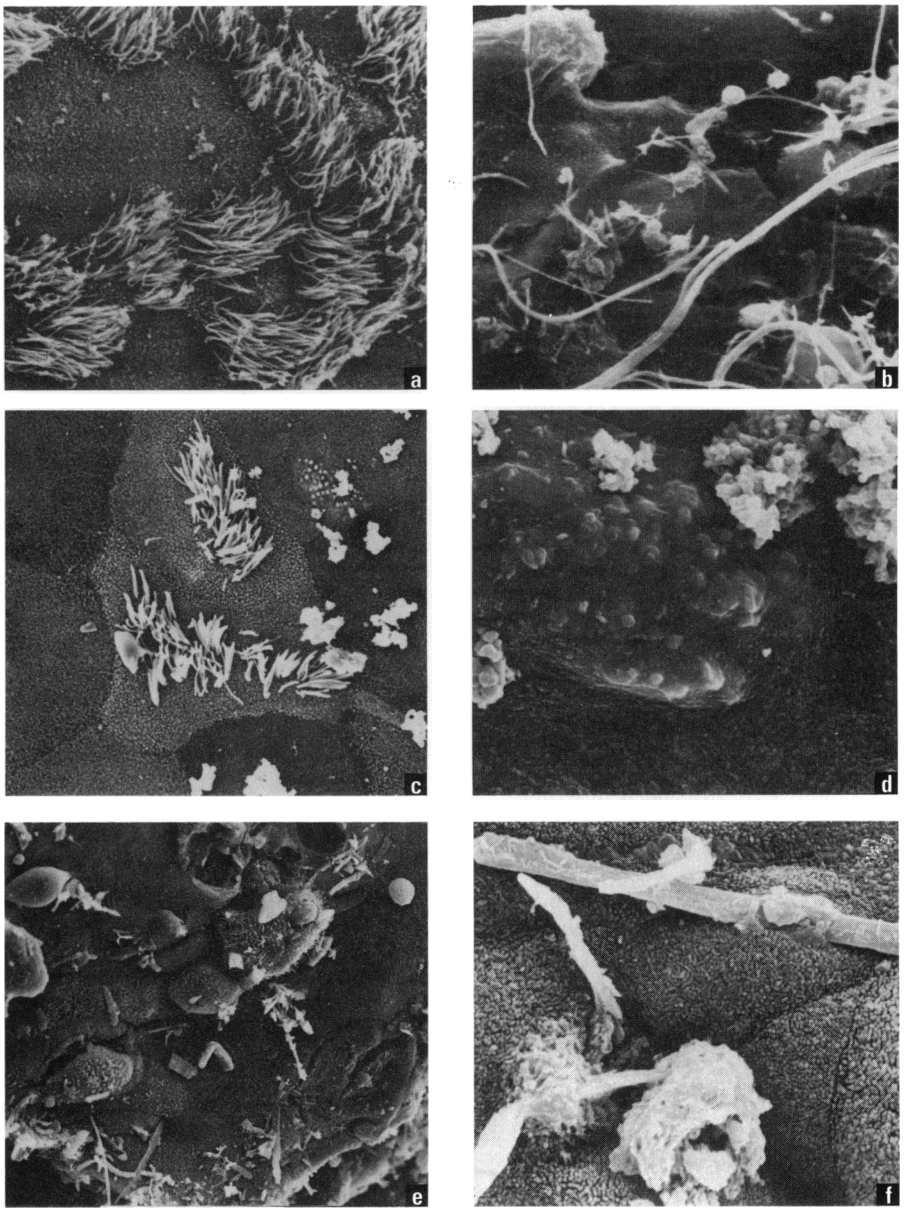

Figure 2. Scanning electron microscopy of rabbit tracheal epithelial cells treated with mineral particles for 3 days after 4 days of culture. (a) Control culture showing a mosaic of ciliated cells and cells with microvilli (1014×). (b) Culture treated with chrysotile at 50 μg/cm^2 for 24 hr. Note the long fibers of chrysotile on the epithelial surface. Some fibers stick into the cells (624×). (c,d) Culture treated with hematite at 100 μg/cm^2 for 24 hr of culture. (c) At low magnification (2028×), clusters of hematite particles appear heterogeneously scattered on cell surface. (d) At high magnification (2964×), inflated cells were observed, suggesting endocytosis of particles. (e,f) Culture treated with nemalite at 100 μg/cm^2 for 3 days. (e) Numerous small, round cells sloughed off the tissue at the periphery of the outgrowth (1560×). Fibers pitted (e) or went across cells (f, 2720×).

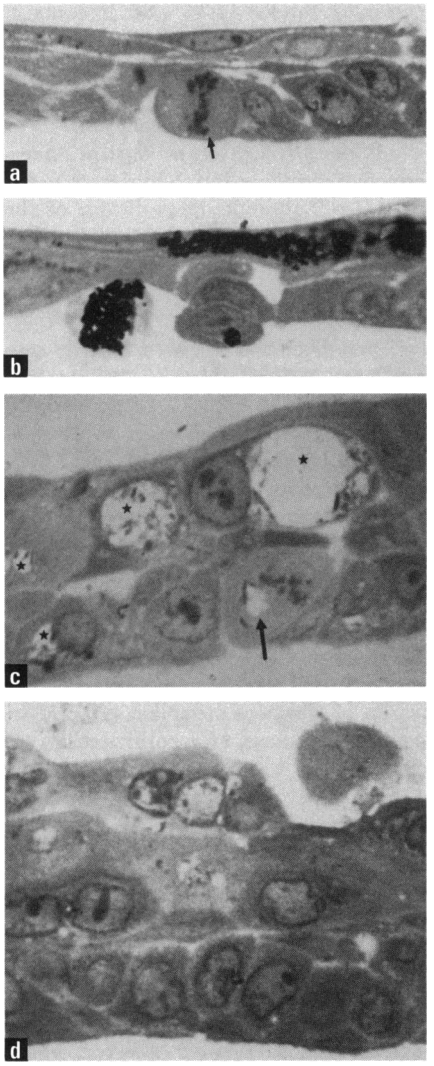

Figure 3. Semithin sections of epon-embedded cultures stained with methylene blue and azur II blue (680×). (a) Control culture after 7 days of culture. Stratified epithelium composed with basal and differentiated cells. Note cell mitosis (arrow). (b) Culture treated by hematite at 50 µg/cm^2 for 3 days after 4 days of culture. Note that both basal and apical cells phagocytosed the particles. (c) Culture treated by nemalite at 50 µg/cm^2 for 3 days after 4 days of culture. Large vacuoles were partially filled with nemalite (star). Note the presence of nemalite in a dividing cell (arrow). (d) Culture treated by chrysotile at 50 µg/cm^2 for 3 days after 4 days of culture. A thickening of the culture was observed and sloughing off the culture.

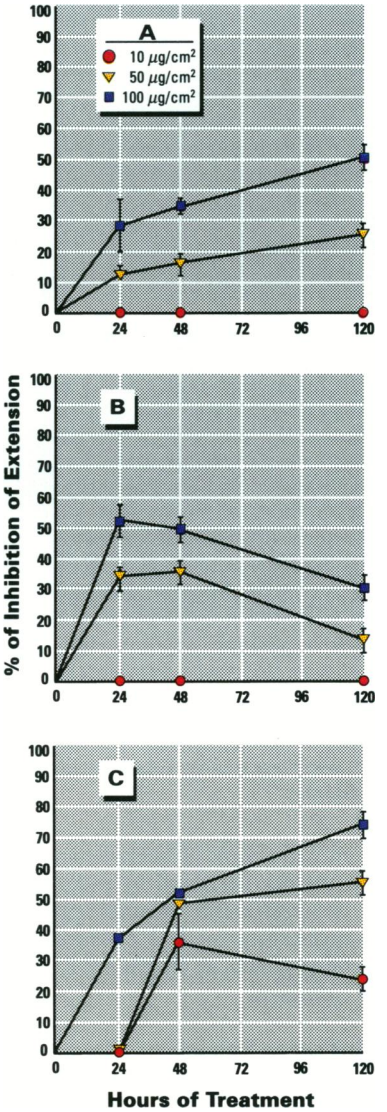

Figure 4. Effects of (a) hematite, (b) nemalite, and (c) chrysotile on culture growth. The particles were applied after 3 days of culture, in a single dose at various concentrations. Inhibition of culture growth was evaluated after different treatment times by the image analysis system and expressed as a percentage of control value. Each point represents the mean of three values ± SE.

of nemalite went across cells, being only partially internalized in the cells (Fig. 2f).

To determine if particles can be phagocytosed by RTE cells, we made semithin sections of treated cultures. Whereas cells near the explant did not exhibit lesions, endocytosis was often noted in cells at the periphery of the outgrowth. Treated cultures exhibited some cells distorted by large vacuoles totally (Fig. 3b) or partially (Fig. 3c) filled with particles. As the cultures were stratified, we can see that basal and apical cells showed phagocytosed particles (Fig 3b,c). As far as the apical cells are concerned, we have never observed endocytosis in ciliated cells. Dividing cells, numerous in the basal layer, may contain phagocytosed particles as revealed by the observations with nemalite (Fig. 3c). In the case of treatment with chrysotile, instead of numerous endocytic cells, numerous round cells exhibiting dramatic lesions and sloughing of the epithelial layer were often observed. Moreover, the outgrowth appeared more stratified as well as the outgrowth treated with nemalite compared to the control culture. About 40% of the peripheral cells are able to phagocytize particles as determined by counting sections of peripheral outgrowth. From these observations we can conclude that all types of particles can be phagocytosed, the round particles of hematite as well as the fibers of nemalite and chrysotile. The size of the fibers was probably a limiting factor. Indeed, we have never observed phagocytosed particles longer than 10 µm (the length of the particles has been determined by measurements from the photos).

Table 1. Effect of mineral particles on viability at 50 and 100 µg/cm^2 for 24 hr of treatment after 7 days of culture

	% of LDH release	Trypan blue (% of viability)
Control	0.93	77.5
Hematite		
50 µg/cm^2	2.51	71.1
100 µg/cm^2	2.03	69.9
Nemalite		
50 µg/cm^2	1.6	73
100 µg/cm^2	ND	69.3
Chrysotile		
50 µg/cm^2	2.65	65.8
100 µg/cm^2	0.65	77.4

Comparison of the results obtained with trypan blue and lactate dehydrogenase (LDH) release. For both tests, values obtained for the treated cultures are not significantly different from the control value, $p < 0.05$ (Student's t-test). ND, not determined.

Acute Toxicity

The effect of hematite, nemalite, and chrysotile on cell viability was evident after 7 days of culture when cells are at the stationary growth phase. Results were shown in Table 1. Regardless of the nature of the particles, after 24 hr of treatment there was not a significant difference of cell viability from the control for the two concentrations tested and with the two tests used.

The effects of hematite, nemalite, and chrysotile on culture growth are illustrated in Figure 4. All particles were tested at three different concentrations for various treatment times. Each type of particle had a dose-dependent effect on culture growth. However, the toxic effect evolved with the time of treatment depending on the type of particle considered.

After 24 hr of treatment, hematite and nemalite had an effect at 50 µg/cm^2 (Fig. 4a,b), and nemalite was more efficient than hematite (33% ± 4 of culture growth inhibition for nemalite compared to the control culture and 12% ± 1.7 for hematite). In contrast, chrysotile only had an effect at 100 µg/cm^2 (37% ± 1.7; Fig. 4c). Considering the short-term effect, nemalite was the most cytostatic particle. Upon classifying the minerals according to their effect on culture growth after 24 hr of treatment at 100 µg/cm^2, nemalite was more efficient than chrysotile, which was more efficient than hematite.

As the cultures were treated, the effect on the growth of the culture evolved. Nemalite had a reversible effect, as recov-

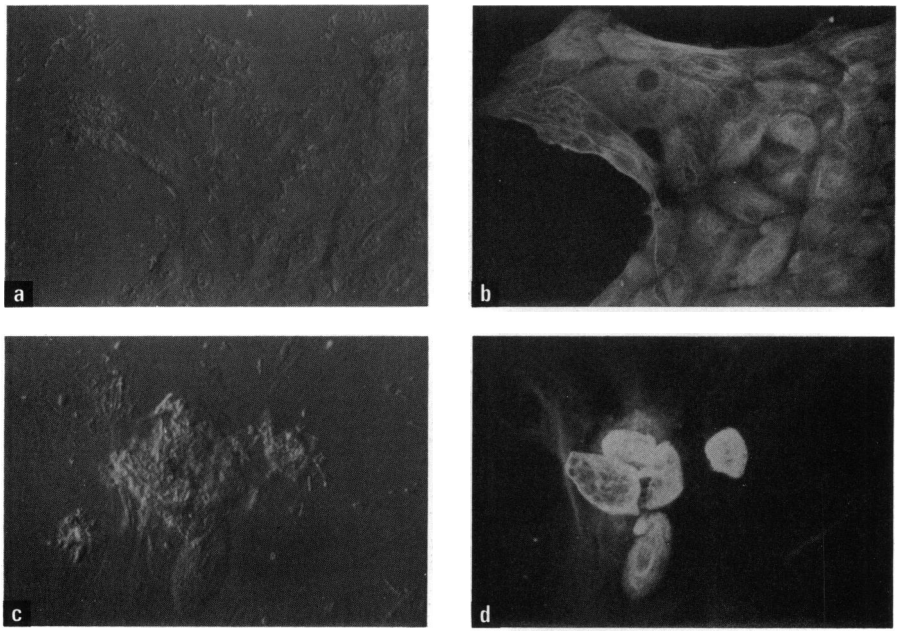

Figure 5. (a–c) Two different 11-day-old cultures of rabbit tracheal epithealial cells treated with nemalite at 20 μg/cm^2 during 7 days (264×). (a) Nomarski interferential contrast observation. (b) Indirect immunofluorescence labeling of keratin network of epithelial cells in culture. Comparing panels a and b, note that the peripheral cells covered with particles exhibit a normal keratin network. (c) Nomarski interferential contrast observation. (d) Indirect immunofluorescence labeling of keratin network of epithelial cells in culture. A comparison of the panels c and d shows that cells exhibiting a dense keratin network correspond to small, round, superficial cells covered or filled with particles.

ery of the growth of the culture was observed after 5 days of treatment even at 100 μg/cm^2. In contrast, the toxicity increase was more conspicuous with the time of treatment from 50 μg/cm^2 for chrysotile and hematite. Considering the long-term effect, chrysotile is the most cytostatic particle. After 5 days of treatment at 100 μg/cm^2, chrysotile was more efficient than hematite, which was more cytostatic than nemalite.

The cytostatic effect observed was initially attributed to mechanical action. Indeed, the peripheral crown of particles could prevent the cells from progressing on the collagen substratum. The inhibition of the culture growth could correspond to a squeezing of the cells rather than to a real inhibition of proliferation. However, two facts allowed us to rule out this possibility. On one hand, recovery of the culture growth can be observed in the cultures treated by nemalite, suggesting that RTE cells were able to get over the particles. On the other hand, the count of cell number according to the outgrowth surface showed that the cellular density was the same in control and treated cultures (data not shown).

The effect of an iron chelator, desferrioxamine, on particle action was investigated. As the direct use of desferrioxamine on RTE cells was cytotoxic, particles were treated for 4 hr with desferrioxamine and then washed with culture medium before their deposition on cell culture. Whereas the cytostatic effect of hematite and chrysotile was not decreased by pretreatment with desferrioxamine, nemalite pretreated with desferrioxamine had a reduced effect on cellular growth at 48.2% ± 9.2 after 24 hr of treatment.

Evolution to Squamous Metaplasia

The ultimate stage of squamous metaplasia is the appearance of CLE beneath the plasma membrane of upper cells. These CLE are insoluble in denaturing and reducing agents. They can be easily counted after cellular dissociation and solubilization. Results summarized in Table 2 show that cultures treated for 13 days with 10 μg/cm^2 of nemalite exhibited a higher number of CLE compared to the number of total cells. The percentage of CLE produced in nemalite-treated RTE cells compared to control cultures is 544% ± 82. In contrast, hematite did not favor the formation of CLE. Chrysotile slightly increased the number of CLE, but the difference is only significant for $p < 0.5$ (Dunnett test).

Table 2. Percentage of cross-linked envelopes (CLE) produced in rabbit tracheal epithelial cells treated at day 3 of culture for 10 days with mineral particles at 10 μg/cm^2 compared to control cultures

Mineral particles	% of CLE × 10^{-3}
Control	1.7 ± 0.7
Hematite	0.6 ± 0.3*
Nemalite	10.95 ± 2.55*
Chrysotile B (UICC)	2.6 ± 1.9*

Results are expressed as the total number of CLE per particle-exposed culture divided by the total cell per particle-exposed culture × 100. Values represent the average of two separate experiments, which both represent the mean of three values. *$p < 0.005$ compared to the control.

As the cytoskeleton of keratins undergoes modifications during squamous metaplasia, we studied the evolution of the cytokeratin network using indirect immunofluorescent staining. Whole cytokeratins were labeled with a polyclonal anticytokeratin antibody.

Even when the cells were entirely covered with particles (Fig. 5a), the cytokeratin network (Fig. 5b) kept an apparently normal structure. However, some cells exhibited a dense network (Fig. 5d). Observation of the same field by Normasky interferential contrast revealed that these cells were covered or filled with particles and sloughed off the culture (Fig. 5c).

Double staining with monospecific monoclonal antibodies allowed us to follow the apparition of squamous cells with the antibody 1C7 specific to cytokeratin-13, a marker of squamous metaplasia (*20, 21*). In the treated cultures, 1C7-positive cells were observed, but the number of these cells was difficult to evaluate only by microscopic observations (data not shown).

To determine whether the expression of cytokeratin-13 was modified in treated cultures, keratins were extracted and separated by 10% SDS-polyacrylamide gel electrophoresis and then transferred onto nitrocellulose. The results of the electrophoresis are shown in Figure 6. Seven main protein bands were observed, which had already been described by Baeza et al. (*21*) as keratin bands. Based on the blue-coomassie-stained gels (Fig. 6a), no obvious differences could be detected between the pattern of keratins of the cultures treated by the particles and the control culture.

The western blots were revealed by monoclonal antibodies, especially against cytokeratin-13. This keratin was expressed both in control culture and treated cultures (Fig. 6b). As the same quantity of protein had been deposited in each well, a greater expression of cytokeratin-13 was observed in the cultures treated with nemalite and chrysotile.

Oxidizing Power of Particles

To determine the oxidizing power of particles, they were suspended in serum-free culture medium supplemented with 1 M phosphate buffer (pH 7.4). We tested their capacity to produce OAS by ESR. We used DMPO to trap the radicals, which would otherwise react too quickly to be detected. The concentration of phosphate in culture medium increased the leaching kinetics of the particles and reinforced, as ligands, the reducing capacity of Fe^{2+}, leading to signif-

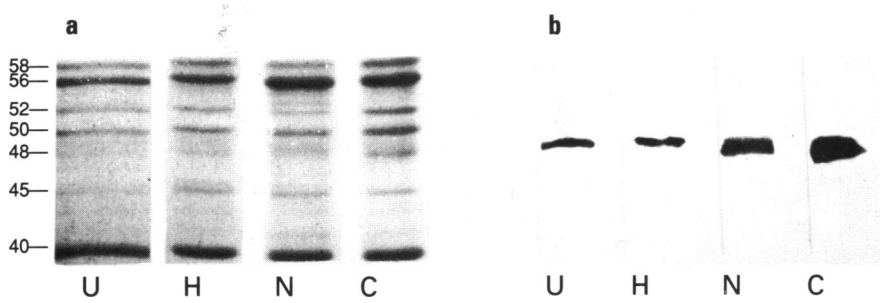

Figure 6. Ten percent sodium dodecyl sulfate-polyacrylamide gel electrophoresis separation of keratin extracted from 10-day-old cultures treated or untreated (U) for 8 days with mineral particles at 50 μg/cm^2: hematite (H), chrysotile (C), nemalite (N). (a) Blue-coomassie-stained gels. Values on the left denote molecular weight (×10^3 kDa). (b) Immunoblot analysis of keratins with the monoclonal antibody 1C7 (antikeratin-13).

icant differences of intensity of the ESR signals. Results presented in Table 3 show that whereas hematite, a ferric oxide, was totally inactive, a significative signal was detected for chrysotile and nemalite.

Table 3. DMPO–$CO_2^{\cdot}$ spin adduct electron spin resonance signal intensities measured after 30 min of incubation of particles

Mineral particles	ESR signal intensity, DMPO–$CO_2^{\cdot}$
Hematite	0-50
Chrysotile B (UICC)	500 ± 50
Namalite	1200 ± 100

Reactions were carried out in serum-free culture medium supplemented with phosphate buffer as described in Materials and Methods. The intensity of the signal was defined in an arbitrary scale. Microwave power was 10 mW, time constant 1 sec and modulation amplitude 3.2 G. An intensity of 1000 in our scale corresponds to 4.10^{18} radicals/l (DMPO-$CO_2^{\cdot}$).

Discussion

The aim of this study was to understand the mechanism of cytotoxicity of some mineral particles on their first target: cells of the upper respiratory tract. In addition to fiber geometry, the oxidation state of the chemical species composing the particle is postulated to play a role in the cellular damage observed after mineral treatment. The effects of three mineral particles containing iron were evaluated in RTE cells.

Morphological studies of RTE cells were first carried out to determine the behavior of the particles in cultures and the resulting structural alterations. As primary cultures of RTE cells reconstituted a mucociliary epithelium with functional ciliated cells, the distribution of particles on the outgrowth quickly became heterogeneous. Peripheral areas of the outgrowth containing few ciliated cells were covered by particles and as a result exhibited cellular modifications. Whatever the morphology of the particle, the three types of particles were phagocytosed by RTE cells. It seems that endocytosis does not depend on the form of the particle. We have shown that particle size must be taken into account in this phenomenon. Studies by Hesterberg et al. (*22*) pointed out the importance of another parameter in phagocytosis: the surface charges. They showed that chrysotile, which has positive charges, is phagocytosed more by rat tracheal epithelial cells than crocidolite which is negatively charged. The presence of positive charges on particle surface facilitates their binding with the negative charges of the membranes and more particularly to sialic acid residues as demonstrated on red blood cells (*23*).

As all morphological observations showed particle-induced lesions, we quantified their toxicity to classify the particles. This evaluation was achieved by membrane permeability assays (a dye exclusion test and lactate dehydrogenase release assay) and culture growth assays. Regardless of the particle, both assays showed no significant membrane damage resulting from a 24-hr particle exposure even at the high concentration of 100 μg/cm^2. This result is in agreement with that obtained by Hesterberg et al. (*22*) for asbestos on rat epithelial cell lines.

The results concerning the growth of the culture show that after 24 hr of treatment, nemalite has the most cytostatic effect at 50 μg/cm^2. A stronger activity of nemalite compared to hematite was also observed on Syrian hamster embryo cells by measuring of the transforming potency (*24*). Nemalite is the most toxic mineral in short-term tests. It also contains a higher proportion of accessible Fe^{2+}. Its toxicity is probably linked to the appearance of Fe^{2+} on its surface as leaching occurs. The appearance of OAS would then be involved in its toxicity. This hypothesis is confirmed by the ESR results. Furthermore, the cytostatic effect of this particle is attenuated by desferrioxamine, an iron chelator. This decrease of nemalite activity by desferrioxamine treatment has already been shown by Fontecave et al. (*25*), studying the lipid peroxidation of liver rat microsomes. Zalma et al. (*26*) have shown that there is inhibition in the formation of OAS after treatment of nemalite by desferrioxamine. For nemalite, after 48 hr, it is probable that the phenomenon of leaching (relatively rapid) is finished and the production of OAS has decreased, possibly explaining the restarting of the culture growth. The effect of hematite on culture growth is weaker than the other two minerals, but it increases with dose and time of treatment. It is possible that the inclusion of hematite particles in vacuoles of cells in the periphery of the culture is accompanied by formation of H_2O_2 in these vacuoles, with the possibility of formation of other oxidizing species by reaction with Fe^{3+}. Pezerat (*5*) emphasized the existence of such species (P*) which are insufficiently oxidative in the presence of the formate anion to allow the appearance of the radical $CO_2^{\cdot}$ but capable of peroxidizing lipids. If this hypothesis is correct, it could explain the slow increase of the inhibition effect with time of treatment with chrysotile (presence of magnetite) and hematite. Lipid peroxidation, by injuring the cellular membranes, could inhibit culture growth. However, phagocytosis, which is more or less important depending on the material concerned, could also play a role in the observed toxicity. This phenomenon should be evaluated by measuring the quantity of phagocytosed particles by cells at different time intervals.

In regard to the concentration used, whatever the particle concerned, a minimum concentration of 10 μg/cm^2 of mineral particles is necessary to observe an effect on culture growth. In contrast, Hesterberg et al. (*22*) determined a CL_{50} of 0.95 μg/cm^2 for chrysotile after 24 hr of treatment to inhibit the cell proliferation of 2C5 cell line of rat tracheal epithelial cells. They worked with a cell line with no functional ciliated cells, which are the cause of a heterogeneous distribution under our culture conditions. Consequently, the particle effect was more homogeneous in Hesterberg et al.'s study than in our outgrowth cells. The heterogeneous distribution caused by the ciliary beat implies that for a theoretical concentration, the particle concentration on the outgrowth is overvalued, whereas the concentration on the peripheral cells is undervalued. Our system of culture better mimics the *in vivo* situation and shows the capacity of the respiratory epithelium to clear away inhaled particles and accumulate them in areas devoid of cilia.

In addition to the cytotoxic effect of mineral particles, their capacity to induce squamous metaplasia is well documented *in vivo* and *in vitro*. These studies were performed on organ cultures that were

treated with particles for several weeks, and squamous metaplasia was principally assessed by morphological observations (*10,27*). In our culture conditions, the short lifetime of primary cultures of RTE cells did not allow treatment of cells for more than 16 days. Therefore, morphological observations linked to the evolution to squamous metaplasia are not always well developed and easily quantifiable. The extent of squamous metaplasia was evaluated by CLE formation in squamous cells. Indeed, Banks-Schlegel et al. (*28*) showed on several human lung tumor cell lines that the extent of envelope formation was well correlated with the degree of squamous differentiation. Nemalite is the only particle able to induce the formation of CLE in significant amounts compared to control cultures. Chrysotile is often mentioned in the literature as an inducer of squamous metaplasia, but under our experimental conditions it did not exhibit a significant difference in the formation of CLE from control cultures. Therefore, keratin analysis was performed to determine the differentiated state of treated cells because it is well known that as squamous metaplasia occurs, cells exhibit a modified keratin pattern, particularly the expression of cytokeratin-13 (*20*). Although control cultures spontaneously express cytokeratin-13, the expression of this keratin is clearly increased in cultures treated with nemalite and chrysotile.

Under our culture conditions, two of the mineral particles tested were able to induce squamous metaplasia. For nemalite, squamous differentiation evolves until its ultimate stage; the formation of CLE. But for chrysotile, the overexpression of cytokeratin-13 appears as the only marker of squamous metaplasia expressed by treated cells. Terminal differentiation is more than likely not reached because of the short time treatment.

Of the three minerals tested, nemalite is the most efficient in producing effects, after a short time of treatment, on the culture growth and the induction of squamous metaplasia. As its action is reduced by pretreatment with desferrioxamine, an iron chelator, and as it produced significant amounts of OAS, we postulate that nemalite acts on RTE cells by oxidative stress linked to its divalent iron content.

Primary cultures of RTE can bring information concerning the effect of particles on airway cells. The functional ciliated epithelium reconstituted *in vitro* is similar to that existing *in vivo*. As such, results obtained are probably more representative of reality than those obtained on cell lines. Moreover, the modification of differentiation by toxic agents can be identified early by two specific criteria. This model appears suitable to study the multistep process of squamous metaplasia and to investigate how particles may alter squamous differentiation control mechanisms leading to neoplastic transformation.

References

1. Stanton MF, Layard M, Tegeris A, Miller E, May M, Morgan E, Smith A. Relation of particle dimension to carcinogenicity in amphibole asbestoses and other fibrous minerals. J Natl Cancer Inst 67:965–975(1981).
2. Hesterberg TW, Barett JC. Dependence of asbestos- and mineral dust-induced transformation of mammalian cells in culture on fiber dimension. Cancer Res 44:2170–2180(1984).
3. Jaurand MC. Observations on the carcinogenicity of asbestos fibers. Ann NY Acad Sci 258–270(1992).
4. Lund LG, Aust, AE. Iron mobilization from crocidolite asbestos greatly enhances crocidolite-dependent formation of DNA single breaks in ØX174 RFI DNA. Carcinogenesis 13:637–642(1992).
5. Pezerat H. The surface activity of mineral dusts and the process of oxidative stress. In: Mechanisms in fiber carcinogenesis (Brown RC, Hoskins JA, Johnson NF, eds), New York: Plenum Press, 1991;387–395.
6. Zalma R, Bonneau L, Guignard J, Pezerat H, Jaurand MC. Production of hydroxyl radicals by iron solid compounds. Toxicol Environ Chem 13:171–187(1987).
7. Bielski BH. Reactivity of hypervalent iron with biological compounds. Ann Neurol 32:28–32 (1992).
8. Barton DH, Doler D. The selective functionalization of saturated hydrocarbons: Gif chemistry. Acc Chem Res 25:504–512(1992).
9. Mossman BT, Eastman A, Landesman JM, Bresnick E. Effects of crocidolite and chrysotile asbestos on cellular uptake and metabolism of benzo(a)pyrene in hamster tracheal epithelial cells. Environ Health Perspect 51:331–335 (1983).
10. Mossman BT. Mechanisms of chemical and physical carcinogenesis in cultured hamster and human tracheobronchial epithelium. In: *In vitro* models of respiratory epithelium (Schiff LJ, ed.), Boca Raton, FL:CRC Press, 1986; 161–182 .
11. Baeza-Squiban A, Romet S, Moreau A, Marano F. Progress in outgrowth culture from rabbit tracheal explants: balance between proliferation and maintenance of differentiated state in epithelial cells. In Vitro Cell Dev Biol 27A: 453–460(1991).
12. Blanquart C, Romet S, Baeza, A Guennou C, Marano F. Primary cultures of tracheal epithelial cells for the evaluation of respiratory toxicity. Toxicol In Vitro 5:449–502(1991).
13. Romet-Haddad S, Marano F, Blanquart C, Baeza-squiban A. Tracheal epithelium in culture: a model for toxicity testing of inhaled molecules. Cell Biol Toxicol 8:141–150(1992).
14. Mossman BT, Craighead JE, MacPherson, BV. Asbestos-induced epithelial changes in organ cultures of hamster trachea: inhibition by retinyl methyl ether. Science 207:311–313 (1980).
15. Mossman BT, Marsh JP, Dantona R, Bergeron M, Senior A. Involvement of active oxygen species (AOS) in injury, repair and proliferation of tracheobronchial epithelial cells after exposure to asbestos fibers. In: Biology, toxicology and carcinogenesis of respiratory epithelium (Thomassen DG, Nettesheim P, eds), Washington, DC:Hemisphere Publishing Corporation, 1990;145–154.
16. Sun TT, Green, H. Differentiation of the epidermal keratinocyte in cell culture formation of the cornified envelope. Cell 9:511–521, (1976).
17. Achtstaetter T, Hatzeld M, Quinlan RA, Parmelee DC, Franke WW. Separation of cytokeratin polypeptides by gel electrophoretic and chromatographic techniques and their identification by immunoblotting. Meth Enzymol 134:355–371(1986).
18. Towbin H, Staehelin T, Gordon J. Electrophoretic transfer of proteins from polyacrylamide gels to nitrocellulose sheets: procedure and some applications. Proc Natl Acad Sci USA 76:4350–4354(1979).
19. Romet S, Schoevaert D, Marano F. Dynamic image analysis applied to the study of ciliary beat on cultured ciliated epithelial cells from rabbit trachea. Biol Cell 71:183–190(1991).
20. Jetten AM, George MA, Smiths HL, Vollberg TM. Keratin 13 is linked to squamous differentiation in rabbit tracheal epithelial cells and down-regulated by retinoic acid. Exp Cell Res 182:622–634(1989).
21. Baeza-Squiban A, Boivieux-Ulrich E, Houcine O, Guennou C, Marano F. Effect of substratum on differentiation of rabbit tracheal epithelial cells in primary culture. In Vitro Cell Develop Biol (in press).
22. Hesterberg WT, Ririe DG, Barett JC, Nettesheim P. Mechanisms of cytotoxicity of asbestos fibres in rat tracheal epithelial cells in culture. Toxicol In Vitro 1:59–65(1987).
23. Brody AR, George G, Hill LH. Interactions of chrysotile and crocidolite asbestos with red blood cell membranes, chrysotile binds to sialic acid. Lab Invest 49:468–475(1983).
24. Elias Z, Poirot O, Pezerat H, Suquet H, Schneider O, Daniere MC, Terzetti F, Baruthio F, Fournier M, Cavelier C. Cytotoxic and neoplastic transforming effects of industrial hexavalent chromium pigments in Syrian hamster embryo cells. Carcinogenesis 10:2043–2052 (1989).
25. Fontecave M, Jaouen M, Mansuy D, Costa D, Zalma R, Pezerat H. Microsomal lipid peroxidation and oxy-radicals formation are induced by insoluble iron-containing minerals. Biochem Biophys Res Commun 173:912–918 (1990).
26. Zalma R. Contribution a l'étude de la réactivité de surface des fibres minérales. Relations possibles avec leurs propriétés cancérogènes (thesis). Paris:Universite P. et M. Curie, 1988.
27. Woodworth CD, Mossman BT, Craighead JE. Squamous metaplasia of the respiratory tract. Possible pathogenic role in asbestos-associated bronchogenic carcinoma. Lab Invest 48:578–584(1983).
28. Banks-Schlegel SP, Gazdar AF, Harris CC. Intermediate filament and cross-linked envelope expression in human lung tumor cell lines. Cancer Res 45:1187–1197(1985).